

Supporting Information for “Glacial runoff modulates 21st century basin-level water availability, but models disagree on the details”

L. Ultee¹, S. Coats²

¹Department of Earth, Atmospheric, and Planetary Sciences, Massachusetts Institute of Technology

²Department of Earth Sciences, University of Hawaii at Manoa

Contents of this file

1. Text S1 to S3
2. Multi-panel figures S2 and S3

Introduction

All analysis shown in the main text is reproducible and extensible for any of the 56 basins using the Jupyter notebook and code we have provided on GitHub (see link in Acknowledgements). We encourage readers interested in detailed results for a specific basin to make use of the material provided there. The public code also allows users to change time scales of analysis—for example, presenting running means over 5-year

Corresponding author: L. Ultee, Department of Earth, Atmospheric, and Planetary Sciences, Massachusetts Institute of Technology, Cambridge, MA 02139 USA. (ehultee@umich.edu)

May 12, 2020, 1:39pm

rather than 30-year windows, or calculating SPEI at a 27-month rather than 15-month timescale—and examine SPEI under the RCP 8.5 rather than RCP 4.5 emissions scenario.

For readers’ convenience, we include below extended results for each of the 56 basins we analyzed, for the same time scales and climate scenario shown in the main text. The results are presented as multi-page sets of panels that replicate the panels shown in Figures 2 and 3 of the main text, but with all 56 basins rather than the 4 examples shown in the text. Figure S2 shows the glacial effect on mean SPEI. Figure S3 shows the glacial effect on SPEI variance. The panels in both figures were computed with climate scenario RCP 4.5, examining SPEI with a 15-month integration timescale, comparing statistics with a 30-year running window.

Text S1. SPEI computation

SPEI is computed by aggregating and normalizing a simple climatic water balance,

$$D_i = P_i - PET_i, \quad (1)$$

where P_i is the precipitation in time step i , PET_i is the potential evapotranspiration in the same time step, and D_i is their difference. We take precipitation P_i directly from the output of each GCM that we analyze. We estimate PET with the Penman-Monteith method, following Allen, Pereira, Raes, and Smith (1998). To calculate PET requires surface temperature, surface pressure, surface specific humidity, and surface net radiation from the GCM. Surface wind is set to be constant, as PET has been shown to be insensitive to the inclusion of surface wind from GCMs (Cook et al., 2014). All methods for calculating PET directly follow those in Cook et al. (2014).

Text S1.1. Sensitivity to integration timescale

SPEI includes a user-selected timescale of integration, which can be adjusted to study different types of drought and different parts of the hydroclimate system. Short timescales relate to availability of water as soil moisture and headwater river discharge, while longer timescales relate to reservoir storage, downstream water discharge, and changes in groundwater storage (Vicente-Serrano et al., 2009). In our analysis, we present SPEI computed with a relatively long integration timescale of 15 months. This choice reflects our focus on hydrological drought in semi-arid mountain basins dependent on frozen precipitation and seasonal snowmelt (see main text section 2 and McEvoy et al., 2012). We also computed SPEI at a range of integration timescales to ensure our results for the 15-month timescale were not anomalous. One example is below; results for all basins and timescales are available on our public repository.

Figure S1 shows the glacial effect on mean SPEI in the Tarim basin (compare with Figure 2b), with SPEI computed at seven different timescales of integration. The qualitative patterns of the glacial effect on SPEI are similar across integration timescales: some models show Δ SPEI increasing nearly monotonically, while others show an initial increase with a peak near midcentury and subsequent decline. Inter-GCM differences in Δ SPEI are broadly consistent across timescales, though the ordering of GCMs from smallest glacial effect in a basin to largest does vary. The magnitude of the glacial effect ranges from 0.1 SPEI units to 2 SPEI units at different timescales. Although the smallest-magnitude effect appears at the shortest timescale of integration in the Tarim basin, there is no monotonic relationship between Δ SPEI magnitude and integration timescale. That is, the magnitude of the effect we analyse does not scale linearly with the SPEI timescale.

Text S2. Accounting for glacial runoff

We account for glacial runoff in each basin during the period 1980-2100 using the runoff simulations of Huss and Hock (2018). Their model is forced by monthly near-surface air temperature and precipitation from global climate reanalysis (Dee et al., 2011) and CMIP5 GCM projections (Taylor et al., 2011), downscaled to each individual glacier. The initial area of each glacier is defined as the “glacier catchment” for the duration of the simulation. That is, the portion of a basin within a glacier catchment does not change over time, even as the area of the glacier itself does change. Runoff is simulated at the individual glacier level and includes all water exiting the catchment, both melted snow and ice as well as rain falling within the catchment boundary. These monthly glacier runoff totals are then aggregated to the basin scale.

In the Huss and Hock (2018) glacial model output, some portion of the GCM-derived precipitation falling within a basin is also counted within the basin glacial runoff. To avoid double-counting precipitation in our SPEI_G moisture source term, we scale GCM-derived precipitation by each basin’s unglaciated area (Equation 1) and add it to glacial runoff scaled by the basin’s glaciated area. PET is then subtracted from this sum, which is equivalent to assuming that both precipitation falling in the unglaciated part of the basin and glacial runoff from the glaciated part of the basin are encountering atmospheric demand for moisture.

Text S3. Quantifying ensemble mean and range

In the present study, we have focused on identifying and interpreting qualitative differences among GCM-projected SPEI with and without glacial runoff. This approach makes

evident, for example, that no one GCM is consistently wetter or drier than another across basins, and that differences in both land and atmosphere schemes shape projected SPEI in glaciated basins (see main text).

Future studies of hydrological drought in glaciated basins may wish to quantify inter-basin differences in the glacial effect. To that end, we have supplied code in our public repository to compute the inter-GCM mean and interquartile range of SPEI for each basin, emissions scenario, and inclusion/exclusion of glacial runoff—the so-called structural uncertainty in the glacial effect. Figure S4 plots these ensemble statistics for the Tarim Basin, both with and without glacial runoff (compare with main text Figure 1). The ensemble mean and interquartile range further reinforce the findings of the main text: without glacial runoff, the Tarim basin would be drying throughout the century, while with glacial runoff conditions are projected to be wetter in the 21st century than the 20th.

References

- Allen, R. G., Pereira, L. S., Raes, D., & Smith, M. (1998). Crop evapotranspiration—guidelines for computing crop water requirements. In *FAO Irrigation and drainage paper* (Vol. 56). United Nations Food and Agriculture Organization.
- Cook, B. I., Smerdon, J. E., Seager, R., & Coats, S. (2014). Global warming and 21st century drying. *Climate Dynamics*, *43*(9-10), 2607–2627. doi: 10.1007/s00382-014-2075-y
- Dee, D. P., Uppala, S. M., Simmons, A. J., Berrisford, P., Poli, P., Kobayashi, S., ... Vitart, F. (2011). The ERA-Interim reanalysis: configuration and performance of the data assimilation system. *Quarterly Journal of the Royal Meteorological Society*,

137(656), 553–597. doi: 10.1002/qj.828

Huss, M., & Hock, R. (2018). Global-scale hydrological response to future glacier mass loss. *Nature Climate Change*, 8(2), 135–140. doi: 10.1038/s41558-017-0049-x

McEvoy, D. J., Huntington, J. L., Abatzoglou, J. T., & Edwards, L. M. (2012). An evaluation of multiscalar drought indices in Nevada and Eastern California. *Earth Interactions*, 16(18), 1–18.

Taylor, K. E., Stouffer, R. J., & Meehl, G. A. (2011). An overview of CMIP5 and the experiment design. *Bulletin of the American Meteorological Society*, 93(4), 485–498. doi: 10.1175/BAMS-D-11-00094.1

Vicente-Serrano, S. M., Beguería, S., & López-Moreno, J. I. (2009). A multiscalar drought index sensitive to global warming: The standardized precipitation evapotranspiration index. *Journal of Climate*, 23(7), 1696–1718. doi: 10.1175/2009JCLI2909.1

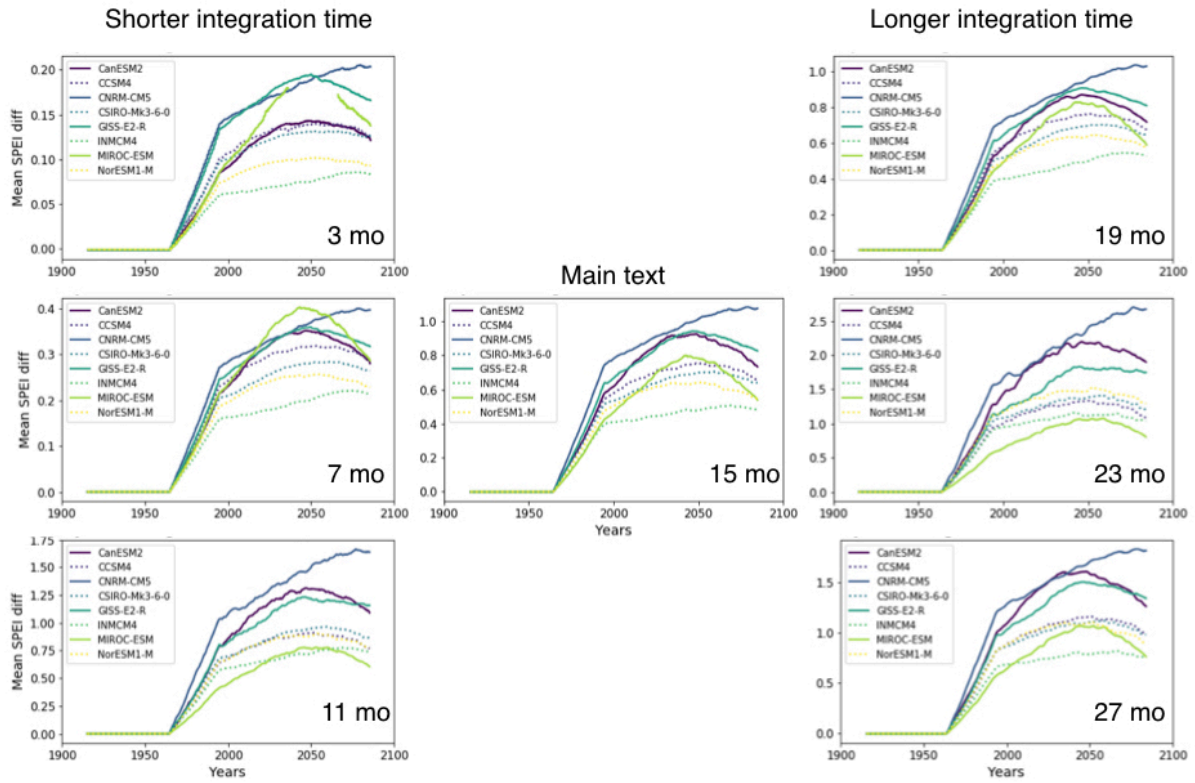


Figure S1. Comparison of glacial effect on SPEI over the 21st century when SPEI is computed with integration timescales ranging from 3 to 27 months. The central panel shows the 15-month integration timescale analysed in the main text of this work; shorter integration timescales appear to the left and longer timescales to the right. Note different y-axis scales in different panels.

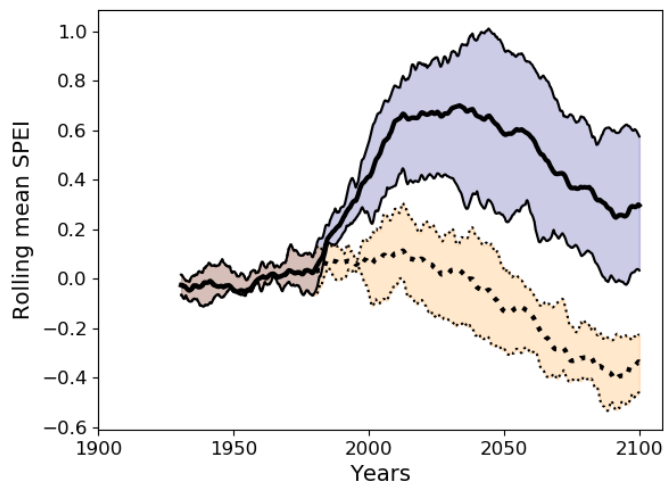


Figure S4. Multi-GCM ensemble mean and interquartile range of SPEI for the Tarim basin, with (solid, blue fill) and without (dashed, orange fill) glacial runoff.